Mapping Ecological Land Systems and Classification Uncertainties from Digital Elevation and Forest-Cover Data Using Neural Networks

P. Gong, R. Pu, and J. Chen

Abstract

Our approaches in this project emphasized mainly the technical aspects of the land-systems classification problem with neural networks. Using digital elevation, its derivatives, and forest cover data as input, we constructed neural networks to classify 27 land-system classes at Duck Mountain, Manitoba, Canada. Training and testing of those neural networks were done using an existing land-systems map prepared through airphoto interpretation and field studies. Two types of data structure were evaluated: polygon and raster forms. Both types of data sets contained the elevation, slope, aspect, dominant forest species and corresponding crown closures, and more general site information on cover type, subtype, site, cutting class, and crown closure. Because the data were obtained from different sources with different scales of measurement, we developed several methods to encode those data into suitable formats for use by the neural networks. With the polygon-based data set, a number of neural network structures and different data encoding methods were tested, and the best overall classification accuracy was only 26.8 percent in agreement with the existing map.

The elevation and the forest-cover data were converted into a raster data set with 50-m by 50-m grid cell units. More experiments were done with this data set. Results indicate that a random sampling strategy for training sample selection led to better classification results than a contiguous sampling method. Approximately 10 percent of the total samples were sufficient for network training. The best overall classification accuracy was 52.0 percent when the neural network classification result was compared with the existing map. We developed a method to estimate classification uncertainties based on neural network outputs obtained from every mapping unit.

Introduction

Mapping ecosystems plays an important role in understanding ecosystem processes and relating these to spatial scales. It has been widely recognized that a hierarchical approach to ecosystems mapping is necessary although levels in a hierarchy and nomenclature vary in different countries (ECOMAP, 1993; Klijn and Udo de Haes, 1994). While ecological maps at broad spatial scales such as ecoregions and ecodistricts are mostly available, maps at more detailed spatial scales have rarely been made. Designing ecosystem classification schemes at small scales such as landscape and land-unit levels requires a great deal of effort for detailed data collection and analysis (e.g., Kojima, 1991; Ohno, 1991; Podani and Feoli, 1991; Ross et al., 1992).

A land system is a unit of land that is mappable at 1: 50,000 scale and distinguishable based on surface form, materials, and hydrology. In the Canadian ecological land system (Wiken, 1985), it corresponds to the ecosection level. A land system can be further divided into forest ecosystem associations with additional information about plant association and soil series (Pedocan Land Evaluation Ltd., 1988). Because forest cover is often a clue to materials and hydrology, it can be used in land-systems classification. Classifying an area into various ecological land systems is usually done using airphoto interpretation and ground observations. It is time-consuming and requires a large amount of expert knowledge to derive land-system classes based on data from multisource such as terrain and land cover. Therefore, efforts have been directed to improve the efficiency of ecological land classification using computer-based digital analysis techniques (Jones, 1993). For example, forest ecosystems classification has been attempted using a knowledge-based approach (Mulder and Corns, 1993). With this technique, expert knowledge must be explicitly acquired and represented in a knowledge base (e.g., Corns and Annas, 1986). However, not only is expert knowledge acquisition difficult and time-consuming, but the computer representation of expert knowledge is also difficult because expert knowledge is often ambiguous and imprecise (Wells, 1992).

Artificial neural network technology is an alternative to constructing a computer system for land systems classification. In such a system, only a set of example data containing the input data and the output classes determined by experts is required (Civco, 1993; Hepner et al., 1990). Expert knowledge does not need to be explicitly acquired. With the learning and adaptive capability of a neural network algorithm, empirical relations between land-systems classes and input data from multisource can be automatically established. It may then be possible to use these relations to conduct land-systems classification. Those empirical relations themselves

P. Gong and R. Pu are with the Department of Environmental Science, Policy, and Management, University of California, Berkeley, CA 94720-3114.

J. Chen is with Hammon, Jensen, Wallen, and Associates, Inc., Oakland, CA 94621-6122.

may be used in the construction of knowledge-based systems. Outputs from a neural network represent the levels of similarity between the characteristics of a mapping unit and those of various land-systems classes. They may be used to estimate classification uncertainties.

The objective of this study was to test the feasibility of applying a back-propagation, feed-forward neural network algorithm to land-systems mapping using digital elevation and forest-cover data. Our emphasis was on the evaluation of the algorithm with various network configurations against input data of different formats with different levels of preprocessing. In addition, we developed a method to estimate uncertainties in land-systems classification using neural network outputs.

The Neural Network Algorithm

A supervised feed-forward neural network was tested in this study. It is capable of classifying data from multiple sources with different levels of measurement scale. This capability cannot be easily accomplished using standard classification techniques (Gong, 1996). A supervised classification method requires classifier training with samples of known classes. Neural network training is achieved by using a generalized delta rule (GDR) (Rumelhart *et al.*, 1986).

The basic elements of a network are nodes and links. Nodes are arranged in layers and linked between two successive layers. Each input node accepts a single value corresponding to an element in an input vector. For land-systems classification, an element in the input vector may be the elevation, aspect, or species crown closure, etc. Each output node corresponds to a class. The value of an output node can be considered as the possibility of a class. Possibilities for all "n" land-systems classes can be arranged in an output vector, $\mathbf{P} = [p_1, p_2, ..., p_n]$. The layers between the input and output layers are hidden layers. The number of hidden layers ranges from one to many, although one is usually enough (Lippmann, 1987; Pao, 1989). The outputs of nodes in one layer are passed to those in the next layer through links that amplify, attenuate, or inhibit such outputs through weighting factors. In the feed-forward neural network model, the input to each node in the hidden layer, or the output layer, is the weighted sum of outputs from the nodes of the preceding layer. The output of a node is calculated from an activation function that usually takes the form of a sigmoid.

During neural network training, both the inputs and the outputs are known. The inputs are a set of attribute values and the outputs are classes of different land systems. The net starts with a random set of weights, taking one input vector at a time and evaluating the output in a feed-forward manner. When presented with an input vector, the net is asked to adjust its weights in all the connecting links and biases in all nodes to generate the desired outputs. The adjustment of weights and biases is accomplished by repetitively feeding the net with vector pairs of inputs and outputs and constantly modifying the weights and biases using GDR. In fact, it is required that the net finds a single set of weights and biases that will satisfy all the input-output vector pairs presented to it.

For each training sample, the error between the desired outputs and the actual network outputs is calculated. With GDR, weights are gradually modified such that the error can be reduced as rapidly as possible. This is done by taking incremental changes that are proportional to the partial derivatives of the root-mean-square error with either the weights or biases. Starting at the output layer, GDR propagates the "error" backward to previous layers, a process known as error back-propagation. This procedure is repeated for all the training samples until either the network outputs for each training sample are very close to the desirable values or the error stabilizes. To construct a neural network, one needs to select representative training samples and to specify the number of hidden layers, the number of nodes in each hidden layer, a learning rate controlling the speed of weight or bias change, and a momentum coefficient controlling the proportion of weights or biases to be preserved from a previous iteration of network training. These parameters are usually determined empirically.

After network training, a set of final weights and a bias for each node will be obtained. With each set of input features, a feed-forward calculation is used to obtain the output values, each of which corresponds to a specific land-systems class. Details about the feed-forward network with the error back-propagation learning algorithm are found in Rumelhart *et al.* (1986), Eberhart and Dobbins (1990), or Pao (1989). A C program has been written to implement this algorithm.

Classification Decision Rule and Uncertainty Modeling

During neural network classification, each set of inputs corresponding to a mapping unit (e.g., a polygon or a grid cell) results in an output vector, P. The neural network assigns a class to the mapping unit according to a maximum possibility rule,

$$\text{assign class } k, \text{ if } p_k = \max\{p_1, p_2, ..., p_n\}$$

i.e., the land-system class for the polygon or the grid cell is the class that has the greatest possibility value among all the possibility values in **P**.

Obviously, the level of uncertainty in each classification decision varies from one polygon (or grid cell) to another. Knowledge about data uncertainty is useful to end users and decision makers (Hunter and Goodchild, 1995; Gong and Chen, 1992; Gong *et al.*, 1995). In particular, classification uncertainties can help the map makers to identify potential problems in original data and the classification scheme design. While these are outside the scope of this paper, we present a method for estimating classification uncertainties.

Intuitively, the uncertainty is related to the maximum possibility, p_k. We may use $1 - p_k$ to represent the uncertainty for the polygon or grid cell under consideration. When p_k approaches 1, the uncertainty level is low. However, some of the remaining possibilities may also be large. From our experience, there usually exist two to three possibility outputs in **P** that are greater than 0.01. Sometimes, both the first and the second greatest possibilities are greater than 0.5. For example, if both the first and the second highest possibilities are close to 0.7. There is a large chance that the class having the second highest possibility is the correct classification. Under such circumstances, the low uncertainty level calculated by $1 - p_k$ seems to be less desirable. Therefore, we included the normalized maximum possibility, $p_k / \sum_{i=1}^{n} p_i$, as a modifying factor in the calculation of the uncertainty level. The uncertainty factor is defined as follows:

$$1 - p_k \cdot p_k / \sum_{i=1}^{n} p_i.$$

This largely increases the level of uncertainty when several high possibilities are generated by the network for a polygon or grid cell.

Study Site and Data Preparation

The study site, covering approximately 240 square kilometres, is located partly inside and partly outside the Duck Mountain Provincial Forest, Manitoba, Canada. Ecological land classification of the same area was conducted using airphoto analysis and ground checked by Pedocan Land Evaluation Ltd. (1988). Twenty-seven land-systems classes were

TABLE 1. THE ECOLOGICAL LAND SYSTEMS CLASSIFICATION SCHEME (ADAPTED FROM THE PEDOCAN REPORT, 1988) AND CODES USED IN TABLE 10.

General Class	Class	Code
Morainal	M1	25
Morainal-Lacustrine	ML1	26
	ML2	27
	ML3	28
Lacustrine-Morainal	LM1	22
	LM2	23
	LM3	24
Stream Channels	SA	2
	SB	3
	SI	1
Glaciofluvial Ridged	FR1	20
Outwash & Beaches	FR2	21
	FB1	12
	FB2	13
Fluvial Fans	F1	9
	F2	10
	F3	11
Bogs	B1	5
	B2	6
	B3	7
	B4	8
Fluvial-Duned	FD1	14
	FD2	15
Fluvial Morainal	FM1	16
	FM2	17
	FM3	18
	FM4	19

Plate 1. Forest-cover map with crown closure of the first dominant forest species.

Plate 2. The Pedocan land-systems classification map.

mapped (Table 1). There exists a large tract of farmland and some water bodies on the map which were excluded from the classification in this study.

Two digital data sources, a digital contour line map and a forest-cover map, were available as input. The first dominant species is shown in Plate 1. UTM grids in kilometre units are also shown in Plate 1. The contour line map was digitized based on 25-foot contour intervals from 1:50,000-scale National Topographic Series maps. The digitized contour map, the forest map, and the Pedocan map (Plate 2) of the Duck Mountain area were provided by the Manitoba District Office, Canadian Forest Service.

In order to apply the neural network algorithm for land-systems classification, the original data were overlaid to form a polygon database and rasterized into a grid file. Both data sets were used in this study.

The Polygon Data Set

Elevation units were converted from feet to metres for the DEM. The contour lines were then interpolated into 50-metre interval because an interval of 25 feet would have led to a database that was too large for subsequent analysis such as building the triangular irregular network (TIN) and polygon overlay. The TIN was established based on the interpolated digital contour map. Slope and aspect information were created for each triangle in the TIN. The elevation, slope, aspect, forest cover, and the ecological land-classification map were overlaid together, resulting in a total of 36,107 polygons. The slope has been classified into ten classes corresponding to $0°$, $-1°$, $1° - 3°$, $3° - 5°$, $5° - 7°$, $7° - 9°$, $9° - 11°$, $11° - 15°$, $15° - 20°$, $20° - 25°$, respectively. Less than 80 polygons having slopes steeper than $25°$ were set to the last slope class. The average for each slope range was used as the slope for a poly-

gon. The aspect was categorized into northeast (NE), southeast (SE), southwest (SW), northwest (NW), and flat (FL). The polygon data set consisted of one polygon layer and one table summarizing all the attribute data and the land-systems class of each polygon. Several examples of the attribute data are shown in Table 2.

Corresponding to each polygon in the overlaid layer was a list of variables including Elevation, Slope and Aspect, three tree species (Sp1, Sp2, and Sp3) and their corresponding percentage crown closures (P1, P2, and P3), a five-digit type aggregate (Cover), and the expert derived ecological land-system class (Land System). The elevation is in metres, ranging from 400 to 850 m. For each polygon there are at most three tree species. They are dominant species in a forest stand recorded with their crown closures in the original forest-cover maps. Eight tree species were found in the study area as dominant species in various forest stands (Table 3). The five digits under "Cover" aggregated the cover type, subtype, site, cutting class, and crown closure of a polygon area, respectively. Cover type has four broad categories: softwood, softwood-hardwood, hardwood-softwood, and hardwood. Subtype indicates species composition under the cover type. It is determined by the proportion of basal area of 2 to 3 main species to the total basal area of all species for a stand. Site classifies land moisture regime into seven classes based on indicator species. Cutting class was grouped into six classes based on merchantable volume per hectare and forest growth conditions. Crown closure was classified based on forest coverage derived from aerial photographs (Manitoba Forestry Branch, undated).

The Raster Data Set
From the TIN, grids with 50-m intervals in both the x and y directions were produced. The elevation z at each grid corner with known (x, y) coordinates was determined through linear interpolation (Figure 1). From the digital forest-cover map, the crown closures for each tree species or the values for each of the five cover types were separated into individual layers. Each of those layers was rasterized using the same grid system as in the TIN.

A surface normal vector was generated for each grid from two elevation gradients along the x and y directions, respectively. Slope, α, and aspect, φ, at the grid cell were derived from the elevation gradients, ∇_x and ∇_y: i.e.,

$$\alpha = \arctan (\sqrt{\nabla_x^2 + \nabla_y^2}),$$
$$\varphi = \arctan (\nabla_x / \nabla_y)$$

where $\nabla_x = \partial z / \partial x$ and $\nabla_y = \partial z / \partial y$. The exact angle of φ is determined by the signs of ∇_x and ∇_y.

No classification or post-processing was applied to the calculated slope values in degrees. The aspect was categorized into northeast (NE), southeast (SE), southwest (SW), northwest (NW), and flat (FL) (Plate 3). A flat surface cell was assigned a value of 400 to distinguish it from the north direction of aspect.

The Pedocan map was also rasterized. The raster data contained 17 grid layers including the elevation, slope, aspect, crown closure for eight tree species, the five cover type digits, and the land-systems class.

Data Encoding
A neural net works better with data ranging between 0 and 1. This requires that some of the numerical data (e.g., Eleva-

TABLE 3. MAJOR FOREST SPECIES IN THE DUCK MOUNTAIN STUDY SITE

Species	Code
Black Spruce	BS
White Spruce	WS
Jack Pine	JP
Balsam Fir	BF
Balsam Poplar	BA
Trembling Aspen	TA
Tamarack Larch	TL
White Birch	WB

tion in Table 2) be compressed or stretched while the thematic data such as aspect be encoded in a numerical range between 0 and 1. A linear compression program was used to find the maximum and minimum values of any input variable and linearly compress or stretch all the variable values to the range of 0 and 1. During network training, each output node must have a value. This could be done by assigning 1 to the node corresponding to the land-system class and 0's to the rest of the nodes.

An overview of the major procedures and various data components is shown in Figure 2. The upper half highlights data preprocessing, data ranges, and procedures used to derive the two types of data sets, while the lower half shows procedures used in neural network training and testing.

Aspect Coding
Two types of coding were applied to aspect for both the polygon and the raster data sets. The first type of coding, Method 1 (Table 6), is shown in Table 4. The aspect was coded using four nodes in the input layer. The encoding method allowed more aspects such as N, E, S, and W to be represented.

The second type of aspect coding, Method 2 (Table 6), required only one input node. This was done based on a statistical analysis of aspect distribution. The occurrence frequency of each aspect with respect to each class, $f(i, j)$, can be enumerated from training samples. i stands for a particular aspect and j denotes a land class. For each aspect, the distribution of frequencies of all classes was related to the level of discriminant power of the aspect. If the frequencies were evenly distributed among all the classes, it implied that a low standard deviation would be generated from those frequencies. This aspect would have little discriminant power in terms of separating the classes. If the distribution of frequencies varied largely from one aspect class to another, this

TABLE 4. ENCODING THE ASPECTS: METHOD 1

	N	E	S	W
NE	1	1	0	0
SE	0	1	1	0
SW	0	0	1	1
NW	1	0	0	1
FL	0	0	0	0

TABLE 2. DATA TYPES AND STRUCTURE

	Input										Output
ID	Aspect	Elevation	Slope	Sp1	P1	Sp2	P2	Sp3	P3	Cover	Land System
217	FL	450	.00	BS	70	TL	20	TA	10	16133	B4
1335	NE	450	.50		0		0		0	44200	FB1
1520	NE	450	.50	BS	40	JP	30	TA	20	14134	FR2
1542	FL	450	.00	BS	40	JP	30	TA	20	14134	FR1

aspect class would have greater separation power for discriminating the classes. This allowed us to assess the discriminant power of aspect *i* (or any other input variable) using its "deviation coefficient," $\delta(i)$, defined by the ratio between the standard deviation and the mean of frequencies for aspect *i*.

Once the aspect having the greatest deviation coefficient is found, we assigned a code of 1 to the aspect for use as the input to neural networks. A code for each of the remaining aspects was assigned as its correlation coefficient with the aspect having the greatest deviation coefficient. Following this rule, a code had been assigned to each of the aspects: NE = 0.11, SE = 0.77, SW = 1.00, NW = 0.75, and FL = 0.19.

Elevation Coding
The first elevation encoding method was to directly compress the elevation to the range of 0 and 1. The second method was to take a logarithm of elevation values and then convert the transformed data into the range between 0 and 1. The logarithm was taken to enhance the details of lower elevation.

Texture measures were also extracted from the elevation data. The first texture measure was edge density. It required three steps to obtain. They were (1) applying a Laplacian filtering to the linearly stretched data, (2) thresholding the edge-enhanced elevation data to obtain an edge-image, and (3) applying average filtering to the edge-image to generate elevation edge density. Details of this approach are found in Gong and Howarth (1990). The three additional texture measures were the homogeneity, dissimilarity, and entropy of elevation. They were obtained based on elevation level co-occurrence enumeration (Jensen, 1996). Textures could be generated from local neighborhoods of different sizes. Without much prior knowledge, we used a neighborhood size of 11 by 11 to generate these textures. Texture extraction was one in a hope to capture local elevation patterns that could be helpful for land-systems classification. For instance, the Pedocan map was prepared based on analyzing the land forms through interpreting airphotos. This included the analysis of local concavity, convexity, location on a slope, etc. With only elevation, aspect, and slope, none of those landform features can be reflected in the neural network classification. Some localized texture features such as the edge-density, dissimilarity, and entropy may represent, to some extent, the local concavity and convexity.

Encoding the Slopes
For the raster data set, slopes were not grouped. We compressed slopes or slope classes to the range between 0 and 1.

Encoding Tree Species
For the forest cover, instead of using the six parameters on species and percentages directly, we represented the eight species by eight nodes in the input layer. The percentage of each species in a polygon or a grid cell was used as the input value to a corresponding node. Because there was a maximum of three species for a polygon or a grid cell, at least five nodes had zero values each time. For each tree species, the cover percentages were compressed to the range between 0 and 1.

Cover Type
For the site aggregate of cover types, the five digits were split and assigned to five nodes. All the values were then compressed to the range between 0 and 1.

Experiments
Different combinations of input variables were examined using neural networks. With the raster data set, the combinations included only elevation data; only topographic varia-

bles including elevation, slope, and aspect data; topographic variables and cover-type data; and topographic data, elevation texture data, species, and cover-type data in land-systems classification.

We tested various neural network structures with different numbers of nodes, different numbers of hidden layers, learning, and momentum rates. By comparing the performances of different neural network configurations, we limited our tests to only a few network configurations. Use of more than one hidden layer did not result in better land-systems classification.

For each data set, we extracted certain portions of samples from the Pedocan map for training. Because of the lack of *in situ* knowledge of the study site, knowledge regarding ecological land-systems classification relies on the Pedocan map. Different sampling strategies for network training were tested. These included random sampling, contiguous sampling, and dividing the study area into two halves by selecting training samples from one half and testing the neural networks using the other half. Overall classification accuracies were calculated by comparing the classification results with either the entire Pedocan map or all the samples except those used for training.

Results

Results from the Polygon-Overlay Based Data Set
From the total of 36,107 polygon records, 2740 samples were selected randomly from each ecological land-systems class. These samples were randomly mixed to form the training samples. The number of input nodes was 19 including the elevation, slope, eight species, five cover types, and aspect coded in four nodes. A single hidden layer was used. Two nets were constructed with 60 and 100 nodes in their hidden layers, respectively. At every 100 iterations of network training, the root-mean-square errors were calculated for the training samples and all the 36,107 samples. The net with 100 nodes in the hidden layer converged faster than that with 60-node hidden layer, measured by the mean-square errors against the number of training iterations. The nets stopped converging after 2000 iterations with an error level of greater than 0.4, much larger than the desired error level of 0.01. The overall classification accuracy was 22.6 percent.

Some additional tests were made with the deviation-coefficient-based aspect coding method. From the total samples, 4658 polygons were selected as training samples. With 50 nodes in the hidden layer, we performed three tests using the topographic features, the five cover types, and eight tree species as network input. The best overall classification accuracy, 26.8 percent, was obtained after 5000 iterations of network training (Table 5). Because the overall classification accuracies were rather poor, no further tests were performed with the polygon data set.

Results from the Raster Data Set

Contiguous Samples for Network Training
Training samples can be selected interactively with the data displayed on a screen monitor. This is a popular method

TABLE 5. RESULTS OBTAINED FROM THE POLYGON DATA SET

Test	η	α	test_accu.(%)	No. iteration
1	0.2	0.6	26.8	5000
2	0.35	0.75	23.6	2000
3	0.6	0.3	10.1	1500

η learning rate
α momentum rate

training sample set. A one-hidden layer network was constructed with 16 input nodes, 50 nodes on the hidden layer, and 27 nodes on the output layer. After testing a few sets of momentum and learning rates, a network with a momentum rate of 0.6 and a learning rate of 0.2 produced relatively fast convergence results. The best overall classification accuracy of 43.0 percent was achieved when the network was trained for 2000 iterations. This test was conducted on a Sun SPARC-20 computer, and it took several days to complete the training. Suspecting that the contiguous sampling strategy may under-represent the data variability of the study site, we decided to use a random sampling method for further analysis.

Random Sample Selection for Network Training
A random sampling program was developed that takes a percentage as input and selects a list of samples out of the total samples according to the percentage specified. Approximately 5 percent, 10 percent, and 20 percent of the total samples were used as training samples. More than 20 neural networks were tested. The primary results are presented below.

(1) Varying the network structure and weight updating parameters
Fixing the number of training samples (8910, approximately 10 percent of the total sample) and using all the remaining samples for test (80,960), we evaluated the effect of network structure and weight update parameters. The number of input nodes (NIN) includes the elevation, slope, eight species, five cover types, and aspect either coded in four nodes or in one node. Some of the better results are listed in Table 6
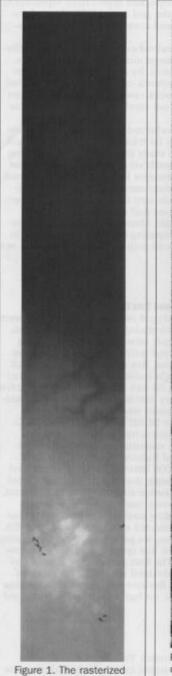

Figure 1. The rasterized elevation of the study area.

Plate 3. The aspect map derived from the digital contour line map.

Figure 2. Data components (in rectangular boxes) and major procedures (in round cornered boxes) used in this study.

adopted in remote sensing image classification. With this method, contiguous patches of samples are usually selected. Each patch contains dozens to hundreds of samples. Approximately 23,000 samples were selected from the total of 87,804 samples for training. To make sure training samples were representative, it was hard to reduce the size of this

Plate 4. The land-systems classification map from a neural network.

Table 7. A small number of training samples (Tests 2 and 3) resulted in comparable classification accuracies. The use of a larger number of training samples (Test 1, approximately 20 percent of the total samples) resulted in a lower classification accuracy. This may indicate that more training is required for some networks. We did not choose to use a larger number of training samples due to the prohibitively high computing cost. The use of approximately 10 percent of the total samples for training (Test 4) resulted in better classification accuracies.

(3) Varying the number of input nodes and hidden layer nodes

Using 8026 randomly selected training samples, the remaining 81,844 samples as testing samples, and a learning rate and a momentum rate of 0.2 and 0.6, respectively, we tested eight neural networks with different numbers of input variables. The best overall classification accuracies are listed in Table 8. The overall classification accuracy with only elevation as network input was 26.8 percent (Test 1). When elevation, slope, and aspect (encoded with the single node method) were used, the best classification accuracy was 35.8 percent (Test 2). This indicates that topographic features contributed a great deal to land-systems classification. When only the five cover types were used, the best accuracy was 20.6 percent (Test 3). When inputs in Tests 2 and 3 were combined, the accuracy was improved to 48.9 percent (Test 4). With the same inputs as in Test 4 but a 30-node hidden layer, the accuracy was 47.8 percent (Test 5). Although the number of hidden layer nodes in Test 5 is only 60 percent of those in Test 4, there is only a 1.1 percent accuracy difference between the two tests. When including the eight tree species in the network inputs, the best accuracy was 52.0 percent (Test 6). Including the eight tree species helped to improve the classification accuracy by approximately 3 percent. When we added the four textures and the logarithm of elevation to the three topographic features and the five cover types (Test 7), the classification accuracy was 50.8 percent, indicating an improvement of 1.9 percent over Test 4. When we used all the inputs in Test 8, the best accuracy was only 51.0 percent, indicating no further accuracy improvement over Test 6. The accuracies for classifying the training samples showed some improvements when including the textures and the logarithm of elevation.

(4) Network training using one half of the study area while testing with the other

The study area was divided into approximately two halves along the middle axial in the vertical direction of the study area as shown in Plate 4. We randomly selected samples from one half and used all the samples in the other half for testing. However, there were only 26 classes in both halves. Therefore, we used 26 output nodes for network testing. Using the three topographic features, five cover types, and eight species as inputs; a hidden layer of 50 nodes; and a learning rate of 0.2 and a momentum rate of 0.6, we made two tests (Table 9). In Test 1, we extracted random training samples from the left half while using the right half as testing samples. In Test 2, the two divisions were exchanged. The test accuracies were less than 33 percent.

Best Overall Classification Results from This Study

The best overall classification accuracy achieved in this study is 52.0 percent. This was obtained using

- 16 input attributes – elevation, aspect, slope, eight tree species, and five cover types;
- one hidden layer with 50 nodes;
- 8026 samples representing approximately 10 percent of the total samples randomly extracted from each class;
- learning rate of 0.2 and momentum rate of 0.6; and
- after 4800 times of network training.

based on 1000 iterations of training. Test No. 3 has the best results.

(2) Varying the sample size

Keeping the number of input nodes to be 16 (with the second aspect coding method), and the number of nodes in the hidden layer to be 50, we tested the effect of training sample size on the classification. Four sets of test results are listed in

TABLE 6. NETWORK TRAINING BY VARYING NETWORK STRUCTURE AND WEIGHT UPDATING PARAMETERS

Test	η	α	NIN	NHN	test_accu(%)	train_accu(%)	No. iterations	aspect coding
1	0.3	0.7	19	40	44.4	47.5	1000	Method 1
2	0.2	0.6	19	50	45.2	48.4	1000	Method 1
3	0.2	0.6	16	50	49.2	51.8	1000	Method 2
4	0.15	0.65	16	30	46.0	48.7	1000	Method 2

η learning rate
α momentum rate
NIN – number of input nodes
NHN – number of nodes in the hidden layer

TABLE 7. NETWORK TRAINING BY VARYING THE TRAINING SAMPLE SIZES

Test	η	α	No train_samp_size	test_accu(%)	train_accu(%)	No. iteration
1	0.2	0.6	17735	45.4	46.9	1000
2	0.1	0.5	4446	46.6	51.1	1000
3	0.2	0.6	4446	45.8	50.7	1000
4	0.2	0.6	8910	49.2	51.8	1000

η learning rate
α momentum rate

TABLE 8. BEST RESULTS OBTAINED FROM THE USE OF DIFFERENT INPUT NODES AND HIDDEN LAYER NODES

Test	NHN	NIN	test_accu(%)	train_accu(%)	No. iteration	Input Variables
1	10	1	26.8	25.8	2425	elevation
2	20	3	35.8	33.6	2075	aspect, elevation, slope
3	25	5	20.6	20.2	1900	5 cover types
4	50	8	48.9	52.1	3500	asp., ele., slope, 5 covers
5	30	8	47.8	49.8	3500	asp., ele., slope, 5 covers
6	50	16	52.0	55.7	4800	input of Test5 + 8 tree species
7	50	13	50.8	56.7	6900	input of Test5 + 5 tansforms of ele.
8	50	21	51.0	57.8	4550	input of Test6 + 5 transforms of ele.

NIN – number of input nodes
NHN – number of nodes in the hidden layer

The confusion matrix for this classification has been calculated (Table 10). The results are shown in Plate 4. Comparing the classification results from the neural network with the Pedocan map (Plate 2), we found through visual inspection that the classes were in general agreement with the Pedocan map. However, the neural network classification results are much fragmented as compared with the Pedocan map.

Classification Uncertainty Map
Figure 3 shows the maximum possibilities of correctly classified grid cells. Grid cells with high possibilities appear bright and low possibilities appear dark in Figure 3. All incorrectly classified cells were assigned 0 and thus they appear black. Figure 4 is the uncertainty map obtained using the proposed method. High uncertainty areas appear bright in Figure 4. It can be seen from Figures 3 and 4 that high uncertainty areas are mostly areas with low maximum possibility values (Portion A) while low uncertainty areas generally have high maximum possibilities (e.g., Portion B). However, this is not always true. Portions C and D indicate that incorrectly classi-

fied areas may not necessarily have high uncertainties. It seems to us that, although the uncertainty map does not highlight all areas where classification was problematic, it is an indicator to most of the areas where classification assignments were questionable.

Discussion
The Pedocan map was prepared based on "(1) surface form and relief, (2) surfacial geological materials, (3) hydrology (position in the watershed and wetness), and (4) dominant forest ecosystems" (Pedocan Land Evaluation Ltd., 1988, p. 29). Dominant forest species were used as indirect features assisting the derivation of the first three types of features. This study was limited by the lack of digital airphotos and ground truth data. Critical information on (2) and (3) is hardly available. The application of the neural networks relied purely on digitized contour lines from 1:50,000-scale topographic maps and digital forest-cover data. In comparison to the airphotos and ground observations, the digital maps (including the Pedocan map) were secondary and were highly generalized. The overall accuracy of 52.0 percent is actually an agreement between the Pedocan map and the neural network classification results. Given the fact that the Pedocan map was used to train the neural networks, we treated it as the "correct" classification of the study area. Although this was not a perfect assumption, the Pedocan map was the best manually derived map prepared by ecologists for that area. Such a map does not exist for most parts of North America.

Rasterizing the original data led to improvements in overall classification accuracies. With the polygon data set,

TABLE 9. RESULTS OBTAINED FROM USING TRAINING SAMPLES FROM DIFFERENT DIVISIONS OF THE STUDY AREA

scheme	NTR	NTT	test_accu(%)	train_accu(%)	No. iterations
1	7061	38822	32.30	44.95	2500
2	6910	43783	28.35	45.83	750

NTR – Number of training samples
NTT – Number of testing samples

TABLE 10. THE CONFUSION MATRIX FOR THE BEST NEURAL NETWORK CLASSIFICATION RESULTS.

	C		L	A		S		S		I		F			I		C	A		T	I			O			N
	1	2	3	5	6	7	8	9	10	11	12	13	14	15	16	17	18	19	20	21	22	23	24	25	26	27	28
1	1125	159	80	0	0	0	0	310	6	0	1	0	0	0	589	50	106	0	0	0	0	0	77	0	13	1	5
2	221	1219	14	0	0	126	0	260	172	16	44	13	0	4	61	4	73	30	138	21	0	0	0	0	0	1	5
3	59	0	1386	48	195	0	0	2	0	0	0	0	0	0	77	102	0	0	0	0	0	0	0	0	0	0	0
5	0	0	80	201	327	0	0	0	0	0	0	0	0	0	0	1	0	0	0	0	200	24	199	238	735	209	41
R 6	0	0	118	14	741	0	0	0	0	0	0	0	0	0	0	0	0	0	0	0	162	2	79	67	540	105	10
7	0	29	0	0	0	4363	48	67	27	73	111	1233	11	790	3	0	6	169	111	16	0	0	0	0	0	0	0
E 8	0	9	0	0	0	245	329	0	1	26	36	404	27	922	0	0	0	47	30	5	0	0	0	0	0	0	0
9	34	68	0	0	0	79	0	4207	99	27	26	0	0	0	63	0	193	6	6	5	0	0	0	0	2	0	0
F 10	10	193	0	0	0	81	19	127	568	41	0	2	0	1	0	0	21	20	102	1	0	0	0	0	1	0	0
11	0	115	0	0	0	174	6	278	91	356	0	1	0	2	11	1	30	21	42	0	0	0	0	0	0	0	0
E 12	0	10	0	0	0	1423	1	0	0	0	1049	1321	86	514	1	0	0	2	139	177	0	0	2	0	0	0	0
13	0	19	0	0	0	595	0	0	21	0	57	2537	0	814	0	0	0	0	41	6	0	0	0	0	0	0	2
R 14	0	0	0	0	0	72	0	0	0	0	2	490	67	121	0	0	0	0	83	0	0	0	0	0	0	0	0
15	0	0	0	0	0	572	36	0	1	0	72	939	33	690	0	0	0	0	43	0	0	0	0	0	0	0	0
E 16	1006	83	119	4	1	14	0	30	0	0	1	0	0	0	4240	229	407	0	0	0	0	0	136	0	36	0	23
17	8	0	25	0	0	0	0	0	0	0	0	0	0	0	228	484	21	0	0	0	0	0	1	0	2	0	4
N 18	144	45	0	0	0	6	0	27	0	19	1	0	0	0	440	55	1809	0	0	3	0	0	0	0	0	0	4
19	1	60	0	0	0	306	10	123	51	28	92	0	0	11	8	0	27	1984	181	241	0	0	0	0	0	0	0
C 20	0	30	0	0	0	129	38	3	1	26	167	318	12	176	0	0	1	47	533	207	0	0	0	0	0	0	2
21	0	1	0	0	0	25	0	0	0	0	203	17	0	6	0	0	0	36	163	1529	0	0	0	0	0	0	1
E 22	0	0	48	104	63	0	0	0	0	0	0	0	0	0	0	0	0	0	0	0	545	4	0	87	236	192	4
23	0	0	184	35	233	0	0	0	0	0	0	0	0	0	0	0	0	0	0	0	303	288	29	52	575	149	0
24	511	0	191	56	54	0	0	0	0	0	0	0	0	0	45	68	0	0	0	0	2	0	1823	5	311	12	152
25	0	0	39	0	19	0	0	0	0	0	0	0	0	0	0	0	0	0	0	0	36	0	0	1138	613	58	0
26	0	0	296	90	369	0	0	0	0	0	0	0	0	0	0	1	0	0	0	0	529	61	80	838	6438	542	12
27	0	0	133	116	360	0	0	10	0	0	0	0	0	0	0	0	0	0	0	0	427	83	65	59	1844	876	52
28	1	0	186	213	38	0	0	0	0	0	0	0	0	0	0	19	0	0	0	0	118	28	76	0	749	28	859

there exists a large number of trivial polygons (spurious polygons) that are too small in size and/or generated by digitization errors. This problem can be reduced in the 50-m by 50-m grid data set. Data for large polygons may be too general because spatial variation within a polygon cannot be captured. The raster data set overcomes this problem to some extent through data interpolation. The 25-foot contour intervals used in the raster data set allowed us to preserve more details in the elevation data. Because the slope and aspect for each cell were generated from the rasterized elevation data, there is more slope and aspect variability preserved in the raster data set than in the polygon data set. The discussion is centered around the following selected aspects.

Effective Neural Network Structure

A neural network with a single hidden layer and a learning rate of 0.2 and a momentum rate of 0.6 worked the best for this study. The number of hidden nodes tested are usually more than twice the number of input nodes, although some tests for geological mapping indicate that this is not necessary (Yang et al., 1996). Our tests indicate that a large difference in number of hidden nodes does not lead to considerably different classification accuracies (Tests 4 and 5 in Table 8).

The close match between training and testing accuracies indicate that 5 to 10 percent of random samples from the total samples for each class were sufficient for network training. This may be further reduced if ground truth data are available. Use of a larger number of training samples requires a longer training time.

Training samples selected from contiguous blocks resulted in relatively lower classification accuracies although a much larger number of training samples was used. Due to the fact that phenomena spatially close to each other tend to be have high auto-correlation, contiguous sampling is less representative than a random sampling if a similar number of samples are selected. In addition, network training within 500 to 1000 iterations seems to be sufficient for evaluation of the potential of a particular network configuration because training errors and testing errors begin to decrease very slowly after 500 training iterations.

Importance of Individual Data Sources to Land-Systems Classification

We used each individual type of input data in land-systems classification. The elevation data are the biggest contributor to the discrimination of the 27 land-systems classes. The three topographic features jointly resulted in an overall classification accuracy of 35.8 percent. The cover aggregates were the second biggest contributor while the crown closures of the eight forest species did not contribute much to the classification. Use of the eight species only produced an overall classification accuracy of approximately 10 percent. It is reasonable to see that the eight species are not as effective as the cover aggregates in land-systems classification. For each mapping unit, the dominant species and their crown closures depict species composition information which accounts for only part of the information provided by the cover aggregate.

As can be seen from Figure 1 and Plate 1, the top portion of the study area is relatively flat with no forest cover. This explained why the classification accuracies are low at that part of the study area. At relatively flat areas, elevation data have less variability and thus have minimal effect on land-systems classification. Under such circumstances, it is

Figure 3. The maximum possibilities obtained by a neural network with correct land-systems classification. A: low maximum possibility area; B: high maximum possibility area; C and D incorrectly classified areas.

Figure 4. The classification uncertainty map. A: high uncertainty area; B: low uncertainty area; C and D: incorrectly classified areas may not necessarily have high uncertainties.

desirable that the forest-cover data as an indirect source of information may help discriminate the land-systems classes. However, forest-cover information is not available for that portion of the study site.

We believe that the discriminating power of the present input variables have been mostly exhausted. Considering that we have only topographic features that are directly related to the land-systems classification while the forest-cover information is only indirectly related, it is possible to further improve the neural network classification using additional data sources such as those on surfacial geology, hydrology, and spatial features that better describe or measure the land forms.

Texture Measures Did Not Help Improve Classification Accuracies in Our Experiment

Most neural networks tested in this study used data only from individual samples by ignoring the spatial relationships among samples. To reduce the inconsistencies in generalization, spatial measures and shape analysis methods may be employed. Although texture measures were tested, the potential of the texture features was not fully explored due to the limitation of data quality and computing power. Texture analysis requires a large amount of computation. On the other hand, the 1:50,000-scale original elevation data do not provide much elevation information at grid cells smaller than 50 m by 50 m. Therefore, micro-relief features finer than 50 m by 50 m with less than 25-foot elevation difference cannot be captured by texture measures. This could be the reason why the use of texture measures did not help improve classification accuracies.

The Neural Network Results Are more Fragmented than the Pedocan Map

Human interpretation of airphotos is a complex abstraction, selection, and generalization process. Computing techniques are far inferior to achieve that level of complexity of intelligent inference. Computing methods are more bounded by data and have poorer generalization capabilities than does the human brain. In this perspective, some of the disagreement between the two maps are caused by inconsistencies of generalization. This is only one part of the problem. Because the quality of any computing method relies heavily on the availability of high quality data, the other part of the problem is related to the data.

By examining the input data, we see that the slope and aspect derived from the digital contour lines have many undesirable artifacts. For example, there are large tracts of contour shaped aspects on the top of the aspect map (Plate 3). With a polygon-based approach, those contour shaped aspects would be the location for many small polygons. These are caused by the drawbacks in restoring the topographic features based on digitized contour lines. Employing digital elevation models extracted from stereo images would considerably eliminate this artifact.

The Neural Networks Failed to Converge

The neural network algorithm is computationally intensive due to the requirement of repetitive network training. With this algorithm, it is impossible to predict when optimal training is achieved. Therefore, we experimented with many different network configurations.

Usually, network training is acceptable when the training error is below a specific small value and the testing error stabilizes. Among all the neural networks tested in this study, the training errors never reached below the specified value of 0.01. All the training errors stopped decreasing at the level of greater than 0.2. We are faced with an insufficient network training problem. Given a large number of

land-systems classes, we believe that the input variables do not have sufficient discriminating power to make network training converge to low training errors.

Training Conducted for One Area Is Less Representative to Another Area

In contrast to the other neural network tests utilized in this study, the testing accuracies were over 10 percent less than their corresponding training accuracies when we experiment with the two halves of the study area (Table 9). This implies that training samples extracted from one area may not be completely representative to the other area even with close proximity. In order to make the neural networks work well for the classification of land systems of different areas, input features that are commonly extractable from different areas and less sensitive to local details should be developed and tested.

Conclusions

From the results obtained in this research, we conclude that

- Adequate input variables are the most important factor to successful land-systems classification. Digital elevation and cover-type aggregate data are more important than dominant forest species and corresponding crown closure data for land-systems classification.
- Organizing input data in a raster data format can produce considerably higher overall classification accuracies than organizing the data in a polygon based format for land-systems classification. Proper encoding of input data helps improve land-systems classification. A deviation-coefficient-based method developed for encoding nominal aspect data helped improve the overall classification accuracies by 3 to 4 percent.
- Random sample selection allowed us to achieve better overall classification accuracies than with the contiguous sample selection method when used for neural network training. Involving more samples in network training may not necessarily lead to better classification results. Approximately 10 percent of samples from each class are sufficient for network training. Decreasing the training samples to approximately 5 percent causes only a 2 to 3 percent drop in overall classification accuracies.
- Changes in the number of hidden layer nodes may not cause much change in overall classification accuracies. The neural network algorithm tested in this research works better with a learning rate and a momentum rate set around 0.2 and 0.6, respectively.
- The proposed classification uncertainty estimation method is capable of highlighting areas where land-systems classification is in question.

Our approaches in this project emphasized mainly the technical aspects of the land systems classification problem with neural networks. Due to the lack of field knowledge, an ecological analysis of the problem such as the appropriateness of the land-systems classes was not attempted. Field knowledge and better understanding of the various classes would help us interpret the classification results. Finding out why some classes were more likely to be misclassified into each other would provide insights on the operational use of the techniques. Further tests and comparisons of different ecological classification schemes would enable us to develop more appropriate land-systems classification methods for the study area.

Acknowledgment

References

Corns, I.G.W., and R.M. Annas, 1986. *Field Guide to Forest Ecosystems of West-Central Alberta*, Northern Forestry Centre, Canadian Forestry Service, Edmonton, Alberta, Canada, 251p.

Civco, D.L., 1993. Artificial neural networks for land-cover classification and mapping, *Int. J. Geographical Information Systems*, 7(2):173–186.

Eberhart, R.C., and R.W. Dobbins (editors), 1990. *Neural Network PC Tools, A Practical Guide*, Academic Press, Inc., Toronto, pp.35–49.

ECOMAP, 1993. *National Hierarchical Framework of Ecological Units*, USDA Forest Service, Washington, D.C., 20 p.

Gong, P., 1996. Integrated analysis of spatial data from multiple sources: Using evidential reasoning and an artificial neural network for geological mapping, *Photogrammetric Engineering & Remote Sensing*, 62(5):513–523.

Gong, P., and J. Chen, 1992. Boundary uncertainties in digitized maps I: Some possible determination methods, *GIS/LIS'92*, San Jose, California, pp. 274–281.

Gong, P., and P.J. Howarth, 1990. The use of structural information for improving land-cover classification accuracies at the rural-urban fringe, *Photogrammetric Engineering & Remote Sensing*, 56(1):67–73.

Gong, P., X. Zheng, and J. Chen, 1995. Boundary uncertainties in digitized maps II: An experiment on digitization errors, *Geographic Information Sciences*, 1(2):65–72.

Hepner, G.F., T. Logan, N. Ritter, and N. Bryant, 1990. Artificial neural network classification using minimal training set, *Photogrammetric Engineering & Remote Sensing*, 56(4):469–473.

Hunter, G.J., and M.F. Goodchild, 1995. Dealing with error in spatial databases: a simple case study, *Photogrammetric Engineering & Remote Sensing*, 61(5):529–537.

Jensen, J.R., 1996. *Introductory Digital Image Processing, A Remote Sensing Perspective*, 2nd Ed., Prentice Hall, Upper Saddle River, N.J.

Jones, R.K., 1993. Next generation forest site classification: ecologically oriented predictive mapping technology, *Proceedings of GIS '93*, Vancouver, B.C., pp. 143–152.

Klijn, F., and H.A. Udo de Haes, 1994. A hierarchical approach to ecosystems and its implications for ecological land classification, *Landscape Ecology*, 9(2):89–104.

Kojima, S., 1991. Classification and ecological characterization of coniferous forest phytogeocoenoses of Hokkaido, Japan, *Vegetatio*, 96:25–42.

Lippmann, R.P., 1987. An introduction to computing with neural nets, *IEEE ASSP Magazine*, pp. 4–24.

Manitoba Forestry Branch, undated. *Guide for Use of Forest Inventory Maps*, Forest Inventory, Forestry Branch, Department of Natural Resources, Province of Manitoba. 21p.

Mulder, J.A., and I.G.W. Corns, 1993. A decision support system for predicting and consolidating ecosystems from existing map data, *Proceedings of GIS'93*, Vancouver, B.C., pp. 153–159.

Ohno, K., 1991. A vegetation -ecological approach to the classification and evaluation of potential natural vegetation of the Fagetea crenatae region in Tohoku, Japan, *Ecological Research*, 6:29–49.

Pao, 1989. *Adaptive Pattern Recognition and Neural Networks*, Addison-Wesley, New York.

Pedocan Land Evaluation Ltd. (Edmonton), 1988. *Forest Ecosystem Classification and Land System Mapping Pilot Project Duck Mountain, Manitoba*, Canadian Forestry Service, Manitoba District Office, Winnipeg, Manitoba, 129 p.

Podani, J., and E. Feoli, 1991. A general strategy for the simultaneous classification of variables and objects in ecological data tables, *Journal of Vegetation Science*, 2:435–444.

Ross, M.S., J.J. O'Brien, and L.J. Flynn, 1992. Ecological site classification of Florida Keys terrestrial habitats, *Biotropica*, 24(4):488–502.

Rumelhart, D.E., G.E. Hinton, and R.J. Williams, 1986. Learning internal representations by error propagation, *Parallel Distributed*

Processing — Explorations in the Microstructure of Cognition, Vol. 1 (D.E. Rumelhart, J.L. McClelland, and PDP Research Group, editors), The MIT Press, Massachusetts, pp. 318–362.

Wells, R.E., 1992. User information needs for forest management site classification in Manitoba, *The Forestry Chronicle*, 68(1):78–84.

Wiken, E., 1985. *Terrestrial Ecozones of Canada*, Lands Directorate, Ecological Land Classification Series, No. 19, 24p.

Yang, G., M.J. Collins, and P. Gong, 1996. Multisource data integration using neural network approach: optimal selection of net variables in lithologic classification, *Proceedings of IGARSS'96*, Lincoln, Nebraska, pp. 2068–2070.

Zogg, G.P., and B.V. Barnes, 1995. Ecological classification and analysis of wetland ecosystems, northern Lower Michigan, USA, *Canadian Journal of Forest Research*, 25:1865–1875.

Forthcoming Articles

Papers listed are scheduled to be published through mid-1997. If you have recently submitted a final version of your paper, it may not have been entered into the print queue yet. If you would like to know when your paper will be published, please send an email to cstaab@asprs.org.

Michael Abrams, Remo Bianchi, *and* Dave Pieri, *Revised Mapping of Lava Flows on Mount Etna, Sicily.*

M. Aniya, H. Sato, R. Naruse, P. Skvarca, *and* G. Casassa, *The Use of Satellite and Airborne Imagery to Inventory Outlet Glaciers of the Southern Patagonia Icefield, South America.*

Ling Bian *and* Eric West, *GIS Modeling of Elk Calving Habitat in a Priairie Environment with Statistics.*

Georges Blaha, *Accuracy of Plates Calibrated by an Automatic Monocomparator.*

M. Les Bober, Duncan Wood, *and* Raymond A. McBride, *Use of Digital Image Analysis and GIS to Assess Regional Soil Compaction Risk.*

Gerardo Bocco *and* Hugo Riemann, *Quality Assessment of Polygon Labeling.*

Michel Boulianne, Clément Nolette, Jean-Paul Agnard, *and* Martin Brindamour, *Hemispherical Photographs Used for Mapping Confined Spaces.*

Timothy L. Bowers *and* Lawrence C. Rowan, *Remote Mineralogic and Lithologic Mapping of the Ice River Alkaline Complex, British Columbia, Canada, Using AVIRIS Data.*

Stefan H. Cairns, Kenneth L. Dickson, *and* Samuel F. Atkinson, *An Examination of Measuring Selected Water Quality Trophic Indicators with SPOT Satellite HRV Data.*

Roland J. Duhaime, Peter V. August, *and* William R. Wright, *Automated Vegetation Mapping Using Digital Orthophotography.*

Christopher D. Elvidge, Kimberly E. Baugh, Eric A. Kihn, Herbert W. Kroehl, *and* Ethan R. Davis, *Mapping City Lights with Nighttime Data from the DMSP Operational Linescan System.*

Patricia G. Foschi *and* Deborah K. Smith, *Detecting Subpixel Woody Vegetation in Digital Imagery Using Two Artificial Intelligence Approaches.*

Jay Gao *and* Stephen M. O'Leary, *The Role of Spatial Resolution in Quantifying Suspended Sediment Concentration from Airborne Remotely Sensed Data.*

Greg G. Gaston, Peggy M. Bradley, Ted S. Vinson, *and* Tatayana P. Kolchugina, *Forest Ecosystem Modeling in the Russian Far East Using Vegetation and Land-Cover Regions Identified by Classification of GVI.*

Clyde C. Goad *and* Ming Yang, *A New Approach to Precision Airborne GPS Positioning for Photogrammetry.*

Qizhong Guo *and* Norbert P. Psuty, *Flood-Tide Deltaic*

Wetlands: Detection of Their Sequential Spatial Evolution.

Collin G. Homer, R. Douglas Ramsey, Thomas C. Edwards, Jr., *and* Allan Falconer, *Landscape Cover-Type Mapping Modeling Using a Multi-Scene Thematic Mapper Mosaic.*

Pamela E. Jansma *and* Harold R. Lang, *Applications of Spectral Stratigraphy to Upper Cretaceous and Tertiary Rocks in Southern Mexico: Tertiary Graben Control on Volcanism.*

Steven T. Knick, John T. Rotenberry, *and* Thomas J. Zarriello, *Supervised Classification of Landsat Thematic Mapper Imagery in a Semi-Arid Rangeland by Nonparametric Discriminant Analysis.*

Jacek Komorowski-Blaszczynski, *Landform Characterization with Geographic Information Systems.*

Miklos Kovats, *A Large-Scale Aerial Photographic Technique for Measuring Tree Heights on Long-Term Forest Installations.*

Sunil Narumalani, John R. Jensen, Shan Burkhalter, John D. Althausen, *and* Halkard E. Mackey, Jr., *Aquatic Macrophyte Modeling Using GIS and Logistic Multiple Regression.*

Paul Pope, Ed Van Eeckhout, *and* Cheryl Rofer, *Waste Site Characterization through Digital Analysis of Historical Aerial Photographs.*

Elijah W. Ramsey III, Dal K. Chappell, *and* Dan G. Baldwin, *AVHRR Imagery Used to Identify Hurricane Damage in a Forested Wetland of Louisiana.*

R.D. Spencer, M.A. Green, *and* P.H. Biggs, *Integrating Eucalypt Forest Inventory and GIS in Western Australia.*

M.D. Tomer, J.L. Anderson, *and* J.A. Lamb, *Assessing Corn Yield and Nitrogen Uptake Variability with Digitized Aerial Infrared Photographs.*

A.P. van Deventer, A.D. Ward, P.H. Gowda, *and* J.G. Lyon, *Using Thematic Mapper Data to Identify Contrasting Soil Plains and Tillage Practices.*

James D. Wickham, Robert V. O'Neill, Kurt H. Ritters, Timothy C. Wade, *and* K. Bruce Jones, *Sensitivity of Selected Landscape Pattern Metrics to Land-Cover Misclassification and Differences in Land-Cover Composition.*

Eric A. Williams *and* Dennis E. Jelinski, *On Using the NOAA AVHRR "Experimental Calibrated Biweekly Global Vegetation Index."*

Paul A. Wilson, *Rule-Based Classification of Water in Landsat MSS Images Using the Variance Filter.*

Zhangshi Yin *and* T.H. Lee Williams, *Obtaining Spatial and Temporal Vegetation Data from Landsat MSS and AVHRR/NOAA Satellite Images for a Hydrologic Model.*

Ding Yuan, *A Simulation Comparison of Three Marginal Area Estimators for Image Classification.*